THE FASEB JOURNAL • RESEARCH • www.fasebj.org

# Transient p53 inhibition sensitizes aged white adipose tissue for beige adipocyte recruitment by blocking mitophagy

**Wenyan Fu,[*,†] Yang Liu,[*,†] Christina Sun,[‡] and Hang Yin[*,†,1]**

[*]Department of Biochemistry and Molecular Biology and [†]Center for Molecular Medicine, The University of Georgia, Athens, Georgia, USA; and [‡]Department of Biological Sciences, Augusta University, Augusta, Georgia, USA

**ABSTRACT: Aging of white adipose tissue (WAT) is associated with reduced insulin sensitivity, which contributes to whole-body glucose intolerance. WAT aging in mice impairs cold-induced beige adipocyte recruitment (beiging), which has been attributed to the senescence of adipose progenitor cells. Tumor suppressor p53 has also been implicated in WAT aging. However, whether p53-related cellular aging in mature white adipocytes is causative of age-impaired WAT beiging remains unknown. It is also unclear whether transient p53 inhibition can rescue WAT beiging. Herein, we report that p53 increased in adipose tissues of 28-wk-old (aged) mice with impaired beiging capability. Cold exposure decreased p53 in beiging WAT of young mice but not in aged mice. In aged mice, inducible p53 ablation in differentiated adipocytes restored cold-induced WAT beiging and augmented whole-body energy expenditure and insulin sensitivity. Transient pharmacological inhibition of p53 led to the same beneficial effects. Mechanistically, cold exposure repressed autophagy in beiging WAT of young mice yet increased autophagy in aged WAT. p53-ablation reduced microtubule-associated protein light chain 3-mediated mitochondria clearance (mitophagy) and hence facilitated the increase of mitochondria during beiging. These findings suggest that p53-induced mitophagy in aged white adipocytes impedes WAT beiging and may be therapeutically targeted to improve insulin sensitivity in aged WAT.—Fu, W., Liu, Y., Sun, C., Yin, H. Transient p53 inhibition sensitizes aged white adipose tissue for beige adipocyte recruitment by blocking mitophagy. FASEB J. 33, 000–000 (2019). www.fasebj.org**

**KEY WORDS: mitochondria · autophagy · aging · insulin sensitivity · diabetes**

Adipose tissues are pivotal for whole-body glucose, lipid, and energy metabolism. White adipose tissues (WAT) store caloric energy in the form of triglycerides and release fatty acids in response to fed/fasted states. In contrast, brown adipose tissue (BAT) dissipates caloric energy by characteristic uncoupling protein 1 (Ucp1)–dependent uncoupled thermogenesis (nonshivering thermogenesis; NST) under cold stress. In rodents, $Ucp1^+$ thermogenic adipocytes (also called beige adipocytes) emerge in WAT depots upon chronic cold stress, sustained sympathetic stimulation or cancer-induced cachexia (1). Recent studies revealed that $Ucp1^+$ adipocytes also coexist with white adipocytes within adult human adipose tissues (2–4). Cold exposure and β3-adrenergic receptor agonists are capable of recruiting and activating $Ucp1^+$ adipocytes in humans, which augments energy expenditure (EE), and improves glucose tolerance and insulin sensitivity (5–8). Thus, stimulating the expansion of beige adipocytes holds promise to restore energy homeostasis in obesity and ameliorate diabetic hyperglycemia.

Recent studies of various human subpopulations revealed an inverse correlation between the activity of $UCP1^+$ beige adipocytes and age (5, 9). This echoes the decline of beige adipocyte recruitment in murine WAT, which starts as early as 4 mo of age (10, 11). The senescence of smooth muscle actin $(SMA)^+$ beige progenitors has been shown to be a cause of age-impaired beige adipocyte recruitment. This is supported by the induced WAT beiging

**ABBREVIATIONS:** Atg, autophagy-related; BSA, bovine serum albumin; Cas9, Caspase 9; *Cidea*, cell death–inducing DNA fragmentation factor–like effector A; CRISPR, clustered regularly interspaced short palindromic repeats; *Cox8b*, cytochrome *c* oxidase subunit 8B, mitochondrial; EE, energy expenditure; *Elovl3*, elongation of very-long-chain fatty acids-3; eWAT, epididymal white adipose tissue; FBS, fetal bovine serum; H&E, hematoxylin and eosin; Hsp, heat shock protein; iBAT, interscapular brown adipose tissue; IHC, immunohistochemistry; IPGTT, intraperitoneal glucose tolerance test; IPITT, intraperitoneal insulin tolerance test; iWAT, inguinal white adipose tissue; KO, knockout; LC-3, microtubule-associated protein light chain 3; mTORC1, mammalian target of rapamycin 1; NST, nonshivering thermogenesis; Pdh, pyruvate dehydrogenase; *Pgc*, peroxisome proliferator-activated receptor γ co-activator; RER, respiratory exchange ratio; ROS, reactive oxygen species; SVF, stromal vascular fraction; Ucp1, uncoupling protein 1; Vdac1, voltage-dependent anion channel 1; $V\text{co}_2$, $CO_2$ production; $V\text{o}_2$, $O_2$ consumption; WT, wild type

[1] Correspondence: The University of Georgia, 325 Riverbend Rd., Center for Molecular Medicine 2228, Athens, GA 30602, USA. E-mail: hyin@uga.edu

doi: 10.1096/fj.201800577R

defect in young *SMA-Cre*$^{ERT2}$*;p21OE* mice and, conversely, the restoration of beiging capability in aged *SMA-Cre*$^{ERT2}$*; Ink4a/Arf*$^{fl/fl}$ mice (11). Besides progenitor-originated *de novo* beige adipocyte differentiation, terminally differentiated white adipocytes in young mice are capable of acquiring the beige adipocyte-specific thermogenic program *via* a transdifferentiation-like mechanism (white-to-beige adipocyte conversion) (12). However, it remains unclear whether the senescence of white adipocytes impairs the white-to-beige adipocyte conversion, and if so, whether this impairment can be alleviated in aged mice to elicit beneficial effects.

Autophagy is an orchestrated degradation process for cellular components (13). In response to the disturbance of mitochondrial functions, mammalian cells undergo microtubule-associated protein light chain 3 LC-3–mediated autophagosome formation surrounding defective mitochondria followed by lysosome fusion and clearance (mitophagy). This process avoids excessive production of reactive oxygen species (ROS) and protects cells from oxidative stress (14). Mitophagy is involved in the mitochondrial remodeling during the maturation stage of adipogenic differentiation (15, 16). Intriguingly, accumulating evidence suggests that the increase of mitochondria during beige adipocyte recruitment requires a dampened mitophagy flux. In support of this view, autophagy-related protein Atg7 ablation in adipose lineage or Myf5$^{+}$ skeletal muscle/brown adipose lineages promotes beige adipocyte recruitment, increases mitochondrial content in WAT, and improves insulin sensitivity (17, 18). Conversely, augmenting autophagic flux by adipose-specific mammalian target of rapamycin 1 (mTORC1) ablation or rapamycin treatment impairs cold-induced beige adipocyte recruitment and impedes the increase of mitochondrial content (19, 20). On the other hand, the conversion of beige-to-white adipocytes in WAT (the reverse process of beiging; also called whitening) upon subdued cold stress is concomitant with a reduction of mitochondrial content and an increase of autophagic flux (21, 22). Blocking autophagy in UCP1$^{+}$ adipocytes by specific ablation of Atg5/Atg12 elongates the maintenance of beige adipocytes in WAT (21). WAT in aged mice has markedly reduced mitochondrial proteins and respiration capacity, which contributes to age-associated obesity (23). Thus, it is conceivable that mitochondrial dysfunction and the consequent increase of mitophagy may negatively impact on the beige adipocyte recruitment in aged mice—a hypothesis that has not been tested thus far, yet has profound clinical implications.

Sustained oxidative stress and the resulting genotoxic responses induce the irreversible cell cycle arrest in stem/progenitor cells (cellular senescence), which leads to deteriorated tissue function and aging. Tumor suppressor p53 plays a crucial role in cellular senescence and tissue aging (24). In aged WAT, increased p53 expression induces the expression of p21 and inhibitor of cyclin-dependent kinase (Ink)-4a/Arf, elevates the release of proinflammatory cytokines, and causes insulin resistance (25). It has been shown that advanced glycation end products (AGEs) can signal through their receptors and reverse the cellular senescence of adipose progenitor cells by impairing p53 signaling and p21 expression (26). Autophagy is also implicated in cellular senescence of progenitor cells. Oncogene-induced cellular senescence is concomitant with the up-regulation of autophagy markers; conversely, inhibition of autophagy impedes the cellular senescence (27, 28). It is noteworthy that p53 has pleiotropic roles in autophagy and mitophagy. Particularly, p53 potentiates autophagy by activating AMPK and repressing mTORC1; the latter is a crucial negative regulator of autophagy (29, 30). Besides, nuclear p53, as a transcription factor, also transactivates many negative regulators of mTORC1, including AMPK β-subunits, tuberous sclerosis complex-2, phosphatase and tensin homolog, and Sestrin-1 and -2, all of which lead to augmented autophagic flux under genotoxic stress or nutrient deprivation (31, 32). On the other hand, it has also been reported that p53 deletion results in extensive mitophagy in many types of tissue and cells (except for skeletal muscle), which can be abolished by a cytoplasmic form of p53 (33). Thus, p53 may have distinct effects on autophagy under various stress and nonstress conditions. Notably, whether p53 plays a role in age-impaired beige adipocyte recruitment and whether this is related to its regulatory function in autophagy and mitophagy remain unknown.

In this study, we found that the beiging capability of WAT correlated with cold-induced p53 repression. Using mouse models of inducible p53-ablation in aged adipocytes and pharmacological inhibition of p53, we showed that transient p53 ablation or inhibition was sufficient to reinstate the beiging capability of aged WAT, which led to augmented EE and improved glucose tolerance and insulin sensitivity. We also provided evidence supporting attenuated autophagy during WAT beiging and potentiated autophagy in aged WAT. Mitophagy markedly decreased in p53-null adipocytes, which was consistent with the increase in mitochondrial content in aged WAT upon p53 ablation. In addition, rapamycin treatment increased mitophagy flux and negated beige adipocyte recruitment in p53 mutants, supporting a causative role of the p53/mitophagy axis in repressing beiging in aged WAT. Thus, this study not only revealed a previously unappreciated beiging defect in aged white adipocytes and the underlying p53-related mechanism but also demonstrated the efficacy of reversing the beiging defect by transient p53 inhibition. These findings may have clinical implications in treating insulin resistance in type 2 diabetes.

## MATERIALS AND METHODS

### Animals

All animal studies were approved by the University of Georgia Institutional Animal Care and Use Committee and performed strictly according to the guidelines. Animals were housed in a temperature-controlled (22°C) environment with 12:12-h light–dark cycle and allowed food and water *ad libitum*. All mouse strains were purchased from The Jackson Laboratory (Bar Harbor, ME, USA): *Adipoq*$^{creER}$ *(024671)*, *p53*$^{flox}$ *(008462)*, *C57BL/6J* (000664). In this study, aged mice were raised to the age of 28 wk compared to young mice of 8 wk. To induce p53 ablation in aged adipose tissues, tamoxifen (100 mg/kg body weight; MilliporeSigma Burlington, MA, USA) was intraperitoneally injected into 28-wk-old *Adipoq*$^{creER}$*;p53*$^{flox/flox}$ mice for 5 consecutive days

and the experiment was conducted 5 d after the last tamoxifen dose. To inhibit the transcriptional activity of p53 in aged mice, we injected p53 inhibitor pifithrin-α (0.44 mg/kg body weight; R&D Systems, Minneapolis, MN, USA) subcutaneously into the inguinal white fat (iWAT) of 28-wk-old mice, 3 times per week for 4 wk. To induce autophagy and mitophagy, rapamycin (2 mg/kg body weight, dissolved in 2% ethanol and 0.9% NaCl; Cayman Chemicals, Ann Arbor, MI, USA) was injected intraperitoneally into 28-wk-old tamoxifen-induced *Adipoq*$^{creER}$;*p53*$^{flox/flox}$ mice for 5 d. Mice were subjected to cold treatment 1 d after the last rapamycin dose.

## Cold exposure

Mice raised at 22°C were exposed to 4°C for cold treatment. For 3 d cold exposure, the following schedule was used: on d 1, mice were exposed at 4°C for 6 h; on d 2, at 4°C for 12 h; and on d 3, at 4°C for a whole day. For 6-d cold exposure, the 3-d cold exposure schedule was followed, and the mice were kept at 4°C after d 3. Food and water were allowed *ad libitum* during the cold exposure.

## Cell culture

Adipose stromal vascular fractions (SVFs) were isolated and differentiated into beige adipocytes. In brief, iWAT was dissected, washed in PBS, minced, and digested with 1.5 mg/ml type II collagenase (Worthington Biochemical, Lakewood, NJ, USA) in isolation buffer [123 mM NaCl, 5 mM KCl, 1.3 mM $CaCl_2$, 5 mM glucose, 100 mM 4-(2-hydroxyethyl)-1-piperazineethanesulfonic acid (HEPES), and 4% fatty-acid-free bovine serum albumin (BSA)] for 45 min at 37°C with frequent agitation. Tissue suspension was filtered through 100 μm cell strainers and centrifuged at 800 *g* for 5 min to pellet SVF. The cell pellet was resuspended in growth medium [high-glucose DMEM containing 20% fetal bovine serum (FBS) and 1% penicillin/streptomycin], plated on collagen-coated cell culture plates, and cultured at 37°C with 5% $CO_2$. Upon confluence, SVFs were induced with induction medium (high-glucose DMEM containing 10% FBS, 0.5 mM isobutylmethylxanthine, 125 mM indomethacin, 2 μg/ml dexamethasone, 1 nM T3, 0.5 mM rosiglitazone, 850 nM insulin, and 1% penicillin/streptomycin) for 2 d and differentiated in differentiation medium (high-glucose DMEM containing 10% FBS, 850 nM insulin, 1 nM T3, 0.5 mM rosiglitazone, and 1% penicillin/streptomycin) for 4 d and the same differentiation medium with 1 mM rosiglitazone for an extra 2 d. For LC-3 staining, cells were treated with chloroquine (50 μM, 18 h; Acros Organic, Bridgewater, NJ, USA) before fixation.

p53 knockout (KO) adipose progenitor cells were generated by a clustered regularly interspaced short palindromic repeats (CRISPR)/CRISPR associated protein 9 (Cas9)–based strategy. In brief, pLentiCrisprV2-p53KO was generated by inserting a p53 sgRNA RNA sequence (sgRNA) (5′-TCTTGTAGATGGCCATGGCG-3′) into pLentiCrisprV2 (52961; Addgene, Cambridge, MA, USA). Lentivirus was packaged by transfecting pLentiCrisprV2-p53KO in 293T cells, and lentiviruses were collected from media after 48 h of transfection. Lentiviruses were used to infect primary SVF cells isolated from aged mice. After 36–48 h of infection, cells were seeded in clonal density and further cultured for 7 d. Control cells with mock lentiviral infection were cultured by the same means. Clones carrying p53-null alleles were confirmed by p53 immunoblot analysis.

## MitoTracker Red

Before staining, the culture medium was removed, and cells were washed with warm PBS. After washing, cells were incubated with 500 nM MitoTracker Red (Thermo Fisher Scientific) in DMEM for 20 min at 37°C with 5% $CO_2$, washed twice with PBS, and fixed by 4% paraformaldehyde at room temperature for 15 min.

## Immunofluorescent staining

Fixed cells were permeabilized with 0.5% Triton X-100 for 15 min, washed twice with PBS, and incubated in blocking solution: 5% normal goat serum (MilliporeSigma) and 1% BSA (Thermo Fisher Scientific) for 1 h at room temperature. Cells were incubated with primary antibodies at 4°C overnight. The primary antibodies used in this study were anti-p53 (2524; Cell Signaling Technology, Danvers, MA, USA) and anti-LC3 (M152-3; MBL, Woburn, MA, USA). After washing, cells were incubated with secondary antibodies (1:250 diluted; Thermo Fisher Scientific). Washed cells were counterstained with DAPI (Thermo Fisher Scientific) and mounted with Fluoroshield reagent (MilliporeSigma). Fluorescence images were acquired on a confocal fluorescence microscope (Olympus, Tokyo, Japan).

## Protein extraction and immunoblot analysis

Tissue lysates were prepared by homogenization in RIPA buffer supplemented with 1× proteinase inhibitor cocktail (Thermo Fisher Scientific). Protein concentration was quantified by bicinchoninic acid assay (Thermo Fisher Scientific). Protein lysates were separated by 10 or 12% SDS-polyacrylamide gels and then transferred to PVDF membrane. The membrane was blocked with 5% nonfat milk/Tris-buffered saline-Tween, probed with primary antibodies at 4°C overnight. After secondary antibody incubation, the membrane was treated with ECL reagents (Thermo Fisher Scientific) and exposed to X-ray films (Santa Cruz Biotechnology, Dallas, TX, USA).

Primary antibodies used in this study were anti-Tubulin (T6199; MilliporeSigma), anti-UCP1 (Ab10983; Abcam Inc., Cambridge, MA , USA); anti-p53 (2524), anti-LC-3 (12741), anti-pyruvate dehydrogenase (PDH) (3205), anti-VDAC1 (4661), anti-HSP60 (4870), anti-COXIV (4850), and anti-PARKIN (4211); and anti-PGC-1α (ST-1202; MilliporeSigma). Secondary antibodies were horseradish peroxidase–conjugated anti-rabbit or anti-mouse antibodies (VWR International, West Chester, PA, USA/Rockland Immunochemicals, Pottstown, PA, USA).

## Real-time quantitative PCR

Total RNA was isolated from tissue or cell culture using Trizol. Total RNA (500 ng) from tissues or cell culture was used in 25 μl reverse transcription reactions (Maxima; Thermo Fisher Scientific) and diluted into 250 μl. Diluted cDNA (2 μl) was used in quantitative PCR reactions (SsoAdvanced Universal Sybr Green mix; Bio-Rad, Hercules, CA, USA) on a Bio-Rad CFX384 Real-Time PCR Detection System. $C_q$ values were determined, and expression values were calculated by Bio-Rad CFX Manager Software. Relative expression values were normalized to inner reference genes ribosomal protein S18 (*Rps18*) and TATA-binding protein (*TBP*) of each biologic sample. Primer sequences are as follows: m*Rps18*_forward: 5′-ACTTCGTGCAAGAAATGCTGA-3′, m*Rps18*_reverse: 5′-TCTGGATTGTTCTTCACTCTTGG-3′; m*Tbp*_forward: 5′-CGCCATGTCTCTAGTGATCC-3′, m*Tbp*_reverse: 5′-GGTCGATGTCTGCTTTCCTC-3′; m*Ucp1*_forward: 5′-ATACTGGCAGATGACGTCCC-3′, m*Ucp1*_reverse: 5′-CGAGTCGCAGAAAAGAAGCC-3′; m*Pgc1α*_forward: 5′-GGTCAAGATCAAGGTCCCCA-3′, m*Pgc1α*_reverse: 5′-TCATAGCTGTCGTACCTGGG-3′; m*Cidea*_forward: 5′-ATACATCCAGCTCGCCCTTT-3′, m*Cidea*_reverse: 5′-ACTTACTACCCGGTGTCCAT-3′; m*Cox8b*_forward: 5′-GAACCATGAAGCCAACGACT-3′,

m*Cox8b*_reverse: 5′-GCGAAGTTCACAGTGGTTCC-3′; m*Elovl3*_forward: 5′-TCCGCGTTCTCATGTAGGTCT-3′; m*Elovl3*_reverse: 5′-GGACCTGATGCAACCCTATGA-3′; m*p21*_forward: 5′-CTTGCACTCTGGTGTCTGAG-3′; m*p21*_reverse: 5′-CAATCTGCGCTTGGAGTGA-3′; m*Bax*_forward: 5′-TGCTAGCAAACTGGTGCTC-3′, *Bax*_reverse: 5′-CTCACGGAGGAAGTCCAGT-3′; and m*Tigar*_forward: 5′-GCCTGGAGGAGAGACAGTT-3′, m*Tigar*_reverse: 5′-TTCCAACAGGGAAAACCTCTG-3′.

### Intraperitoneal glucose tolerance test

An intraperitoneal glucose tolerance test (IPGTT) was performed in mice after 16 h food withdrawal. Glucose (2 g/kg body weight) was injected intraperitoneally. Blood samples were taken from the tail vein. Glucose levels were measured with a glucometer (OneTouch, Ultra 2; LifeScan, Milpitas, CA, USA) at 0, 15, 30, 60, and 120 min after glucose injection.

### Intraperitoneal insulin tolerance test

An insulin tolerance test (IPITT) was performed in mice after 6 h food withdrawal. Insulin (0.75 U/kg body weight; Roche, Risch-Rotkreuz, Switzerland) was injected intraperitoneally. Blood samples were taken from the tail vein. Glucose levels were measured with the glucometer at 0, 15, 30, 60, and 120 min after insulin injection.

### Indirect calorimetry

Indirect calorimetry was performed on a Comprehensive Lab Animal Monitoring System (CLAMS; Columbus Instruments, Columbus, OH, USA) equipped with 8 metabolic cages. Oxygen consumption ($Vo_2$; mm/min) and carbon dioxide production ($Vco_2$; mm/min) were measured at 22°C with 12-h dark–light cycles. Total EE was estimated with an equation published by Lusk in 1928 (34). Data were normalized to the body weight of each animal. Physical activity is measured by counting infrared beam breaking events.

### Hematoxylin and eosin staining and immunohistochemistry

For histology, iWAT was excised from mice and fixed with 10% formalin, dehydrated, and embedded in paraffin. The sliced tissue (5 μm) was stained with hematoxylin and eosin (H&E) (MilliporeSigma). Cell size was quantified by ImageJ [v.1.47t; National Institutes of Health (NIH), Bethesda, MD, USA]. Alternate sections were used for immunohistochemistry (IHC) of UPC1 and H&E staining. Paraffin-embedded sections were antigen unmasked with Tris-EDTA buffer [10 mM Tris Base, 1 mM EDTA, and 0.05% Tween 20 (pH 9.0)] at 93°C for 15 min. Sections were blocked with blocking solution (10% normal goat serum and 1% BSA in PBS) for 1 h at room temperature and incubated with the primary antibody (anti-UPC1, 1:200 diluted in blocking solution) overnight at 4°C. The endogenous peroxidase was quenched with 3% hydrogen peroxide. Sections were incubated with the secondary antibody for 1 h at room temperature. Slides were developed with DAB (Vector Laboratories, Burlingame, CA, USA) for 5 min followed with hematoxylin counterstaining for 1 min. Color images were captured on a DM4000B microscope equipped with a DFC450c camera (Leica, Microsystems, Deerfield, IL, USA).

### Statistical analysis

All data in the figures are expressed as means ± SEM with ≥3 biologic replicates. Statistical significance was determined by Prism 6 (GraphPad, La Jolla, CA, USA) with the unpaired, 2-tailed Student's *t* test. Values of $P < 0.05$ were significant.

## RESULTS

### Increased p53 expression and impaired beige adipocyte recruitment in aged WAT

We first compared p53 expression levels in iWAT and epididymal white adipose tissues (eWATs) of young (8-wk-old) and aged (28-wk-old) *C57BL/6* mice. In both iWAT and eWAT, p53 protein increased in aged mice compared to young mice (**Fig. 1*A***). Like the WAT, p53 also increased in interscapular brown adipose tissue (iBAT; data not shown). It has been reported that p53 expression increases in macrophages and endothelial cells in aged tissues (35, 36). To confirm p53 increased in adipocytes of aged iWAT/eWAT, we isolated SVF from iWAT of young and aged mice and examined p53 expression in cultured adipocytes differentiated *in vitro*. p53 immunofluorescence staining revealed elevated p53 expression in the adipocytes derived from aged mice, compared to those derived from young mice (Fig. 1*B*). The weak p53 signal in the adipocytes derived from young mice was virtually localized in the cytoplasm, whereas p53 was exclusively present in the nucleus of the adipocytes derived from aged mice (insets). The nuclei of aged adipocytes were apparently larger than those of young adipocytes. Thus, p53 was not only expressed at a higher level in aged adipocytes but also was enriched in the nucleus, suggestive of its potentiated transcriptional regulation function in aged adipocytes.

Next, we examined the beige adipocyte formation in iWAT of young and aged mice that were housed at room temperature (22°C) or had been exposed to cold (4°C) for 3 d. In 8-wk-old mice, Ucp1, a marker of thermogenic beige adipocytes, was expressed in iWAT at 22°C (a temperature below the thermoneutrality threshold of mouse and hence presents as a mild cold stress; Fig. 1*C*). In line with cold-induced WAT beiging, Ucp1 increased in iWAT of young mice after 3 d of cold exposure. In clear contrast, Ucp1 was not detected in iWAT of aged mice at either 22°C (mild cold) or 4°C (severe cold), suggesting defective beige adipocyte recruitment in 28-wk-old mice. iWAT of aged mice contained adipocytes of increased size at 22°C, compared to iWAT of young mice (Fig. 1*D*). After cold exposure, iWAT of young mice contained many small adipocytes with multilocular droplets, morphologically resembling beige adipocytes. In contrast, although most adipocytes became smaller, multilocular adipocytes were virtually absent in iWAT of cold-treated aged mice. Thus, compared to young mice, iWAT in aged mice had impaired beige adipocyte recruitment under mild cold or severe cold (3 d).

### Induced p53 ablation in aged white adipocytes reinstated beiging capability after cold exposure

The coincidence of increased p53 expression and impaired beiging capacity in aged mice intrigued us to investigate

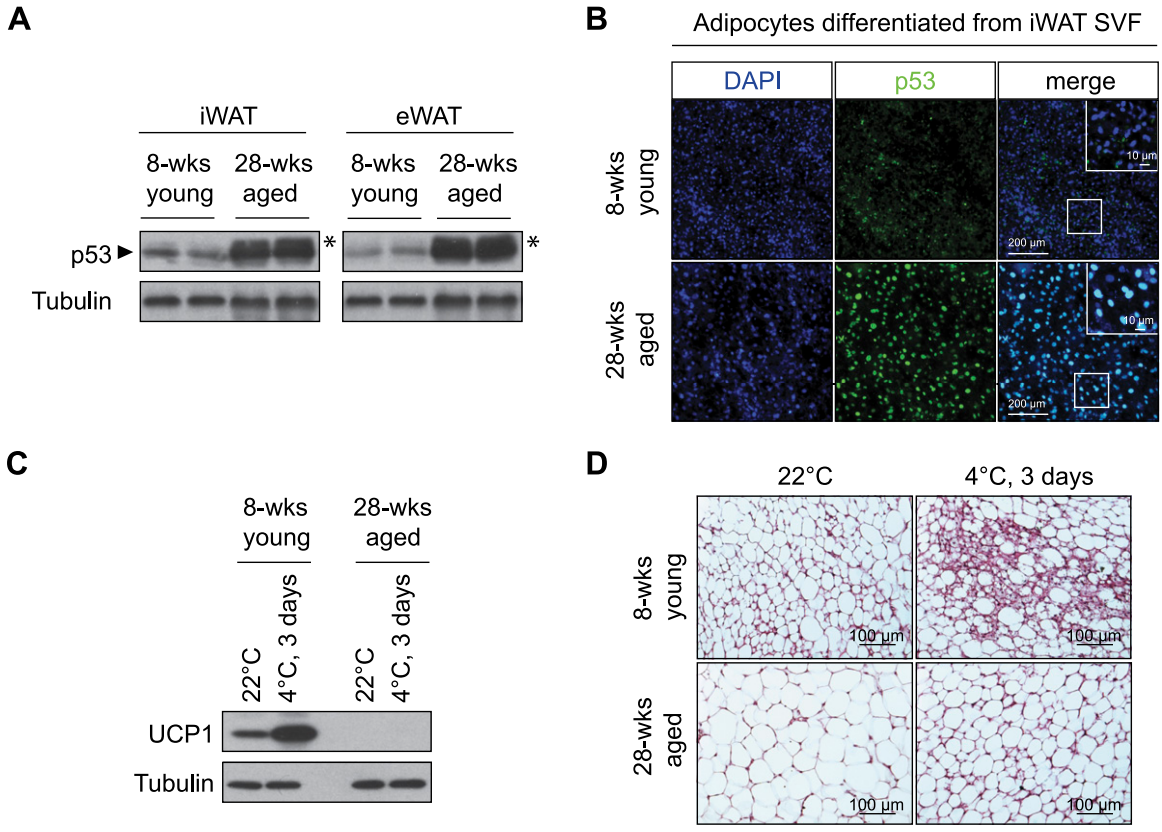


**Figure 1.** Increased p53 expression and impaired beige adipocyte recruitment in aged WAT. *A*) Immunoblot analysis of p53 in iWAT and eWAT of young (8-wk-old) and aged (28-wk-old) *C57BL/6J* mice. Arrowhead indicates p53 bands. Asterisk denotes nonspecific bands with higher apparent molecular weights. *B*) Immunofluorescence staining of p53 (green) and DAPI counterstaining (blue) in cultured adipocytes differentiated from SVFs of young and aged iWAT. *C*) The expression levels of Ucp1 in iWAT of young and aged *C57BL/6J* mice at 22 and 4°C (3 d). *D*) H&E staining of iWAT of young and aged mice at 22 and 4°C (3 d).

whether the expression of p53 is under regulation during WAT beiging in young mice. Cold exposure (4°C, 6 d) decreased p53 expression in both iWAT and eWAT of young mice, whereas p53 expression remained unchanged in aged iWAT under the same condition (**Fig. 2*A***).

To test whether the reduction of p53 expression might be instrumental to beiging in aged WAT, we generated inducible adipocyte-specific p53 KO mice (*Adipoq*$^{creER}$;*p53*$^{flox/flox}$). Previous studies demonstrated that constitutive p53 KO protects mice from cellular senescence in adipose tissues (25, 37). However, it remains unclear whether the antiaging effect is related to adaptations to long-term p53 loss of function. Inducible *Adipoq*$^{creER}$;*p53*$^{flox/flox}$ mice allowed us to determine the short-term effect of p53 loss on WAT aging. Tamoxifen was administered to aged *Adipoq*$^{creER}$;*p53*$^{flox/flox}$ mice (28-wk-old) to induce recombination and p53 KO in differentiated mature adipocytes (hereafter called Adipoq-p53iKO mice; Fig. 2*B*). Tamoxifen-injected *p53*$^{flox/flox}$ littermates were used as the control. To study effects of p53 ablation on WAT beiging, Adipoq-p53iKO and control mice were exposed to cold (4°C) for 3 or 6 d or remained at room temperature. One week after tamoxifen administration, as expected, aged Adipoq-p53iKO mice had reduced p53 expression in iWAT, eWAT, and iBAT (Fig. 2*C*). The residual p53 expression in Adipoq-p53iKO mice may reflect the reported increases of p53 in adipose progenitor cells, macrophages, and endothelial cells (26, 35, 36), which are not affected by *Adipoq* promoter-driven Cre expression in differentiated adipocytes (38). RT-qPCR also confirmed reduced expression levels of known p53 target genes [*Cdkn1a* (or *p21*), *Tigar*, and *Bax*] in aged iWAT of Adipoq-p53iKO mice, compared to the control (Fig. 2*D*). To investigate whether short-term p53 ablation affects beiging in aged WAT, we performed RT-qPCR for *Ucp1*, *Pgc1a*, cell death–inducing DNA fragmentation factor–like effector A (*Cidea*), cytochrome *c* oxidase subunit 8B (*Cox8b*), and elongation of very-long-chain fatty acids-3 (*Elovl3*), which are selectively expressed in beige adipocytes, but not in white adipocytes. At 22°C, all of the above beige adipocyte markers were expressed in significantly higher levels (1.6–4-fold higher) in iWAT of aged Adipoq-p53iKO mice compared to control aged littermates (Fig. 2*E*). After exposure to 4°C for 3 d, aged Adipoq-p53iKO mice also had higher mRNA levels (2–5-fold higher) of *Ucp1*, *Pgc1α*, *Cidea*, *Cox8b*, and *Elovl3* in iWAT compared to control aged littermates. This result suggests that short-term p53 ablation potentiated beige adipocyte formation in aged WAT. In line with mRNA levels of beige adipocyte markers, Ucp1 protein was not detected in either aged iWAT or eWAT of cold-exposed (4°C, 3 d) control mice yet was expressed in iWAT of cold-exposed aged Adipoq-p53iKO mice (Fig. 2*F*). After

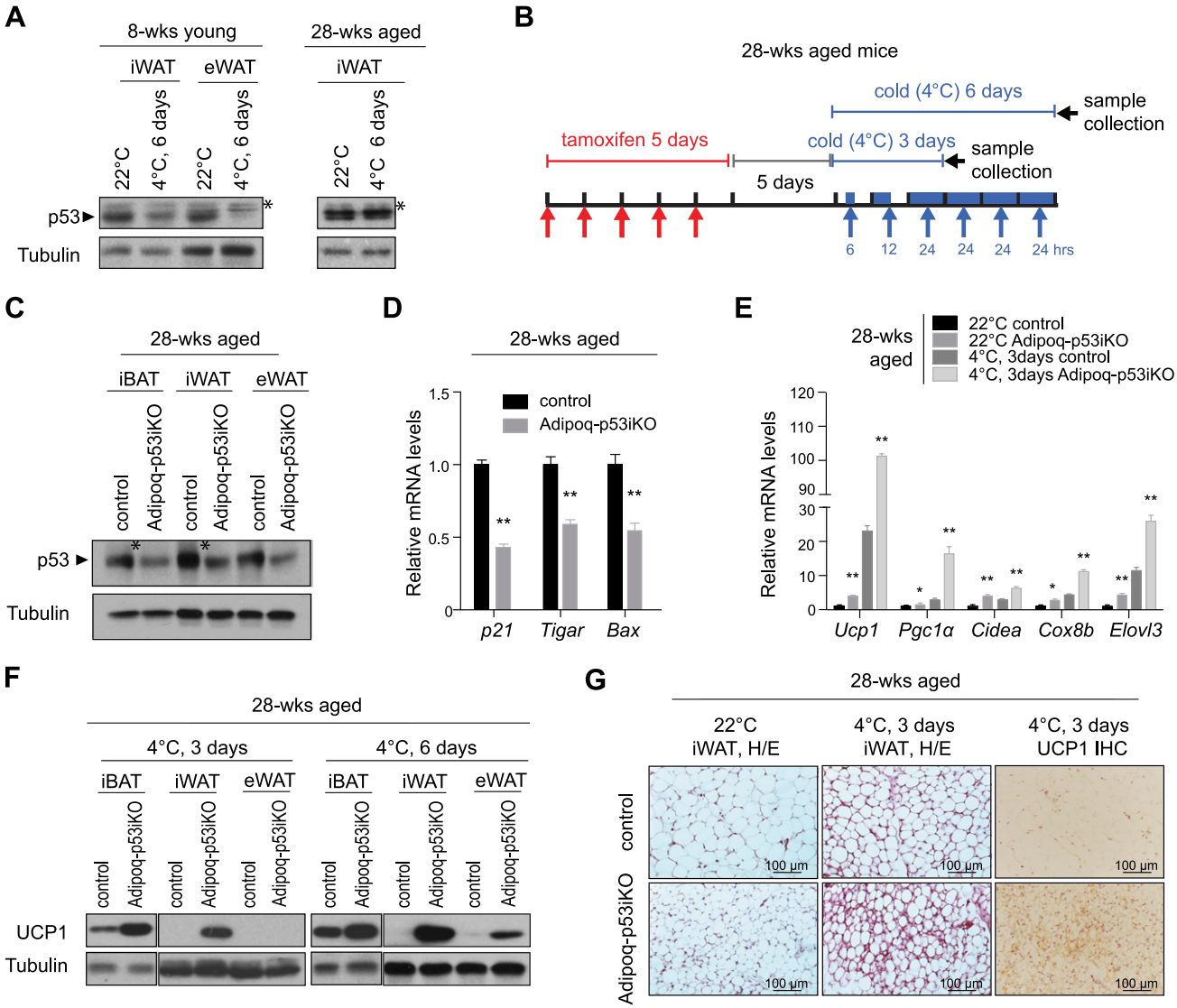


**Figure 2.** p53 ablation in aged white adipocytes reinstated beiging capability. *A*) The expression levels of p53 at 22 and 4°C (6 d) in iWAT and eWAT of young *C57BL/6J* mice and in iWAT of aged *C57BL/6J* mice after 4°C (6 d) exposure. *B*) Experimental design of inducible p53 ablation in adipose tissues of aged Adipoq-p53iKO mice and control littermates. The timing of tamoxifen injection (red arrows), cold exposure (blue rectangles), and tissue collections (black arrows) were indicated on a time axis. *C*) Immunoblot analysis of p53 in iBAT, iWAT, and eWAT of Adipoq-p53iKO mice and control littermates after 4°C exposure for 3 d. Arrowhead: p53 bands; asterisk: nonspecific bands with higher apparent MW. *D*) Relative mRNA levels of p53 target genes *p21*, *Tigar*, and *Bax* in iWAT of aged Adipoq-p53iKO mice and control littermates 7 d after tamoxifen administration (22°C). *E*) Relative mRNA levels of beige adipocyte markers *Ucp1*, *Pgc1α*, *Cidea*, *Cox8b*, and *Elovl3* in iWAT of aged Adipoq-p53iKO mice and control littermates at 22°C or after 4°C cold exposure for 3 d. *F*) Immunoblot analysis of Ucp1 in iBAT, iWAT, and eWAT of aged Adipoq-p53iKO mice and control littermates after 4°C exposure for 3 or 6 d. *G*) Ucp1 immunohistochemistry and H&E staining of iWAT of aged Adipoq-p53iKO mice and control littermates in 22°C or after 4°C cold exposure for 3 d. Means ± SEM, by statistical analysis software using unpaired, 2-tailed Student's *t* test; n.s., not significant (*D*, *E*). $*P < 0.05$, $**P < 0.01$.

exposure to cold for 6 d, Ucp1 was notably expressed in both aged iWAT and eWAT of Adipoq-p53iKO mice, yet was still undetectable in control aged mice. As in WAT, p53 ablation also increased Ucp1 expression in aged iBAT after cold exposure. In parallel with the increase of Ucp1 expression, multilocular Ucp1$^+$ beige adipocytes were observed in iWAT of aged Adipoq-p53iKO mice after 3 d of cold exposure; however, these cells were virtually absent in control mice under the same condition (Fig. 2*G*). At 22°C, the size of adipocytes in iWAT of aged Adipoq-p53iKO mice was smaller than that of control mice and resembled the morphology of adipocytes in young mice (Fig. 2*G* *vs.* Fig. 1*D*). These support the notion that short-term p53 ablation in aged WATs is sufficient to reinstate beige adipocyte formation.

## p53 ablation in aged adipose tissues augmented EE, reduced adiposity, and improved insulin sensitivity

Next, we investigated whether adipose-specific p53 ablation in aged mice affects whole-body energy homeostasis and glucose metabolism. Beige adipocyte recruitment in WATs usually results in increased EE (39). Indirect

calorimetry revealed that aged (28-wk-old) Adipoq-p53iKO mice had increased total EE, $Vo_2$, and $Vco_2$ in both light and dark cycles, compared to control aged mice (**Fig. 3*A*–*C***). The respiratory exchange ratio (RER) of aged Adipoq-p53iKO mice was lower than the control mice in light cycles (Fig. 3*D*), indicative of augmented fatty acid oxidation. The physical activity of both groups of mice was comparable (Fig. 3*E*). Adipoq-p53iKO and control mice had comparable total body weight within 10 d after p53 ablation, when indirect calorimetry was performed (Fig. 3*F*). However, iWAT and eWAT depots of aged Adipoq-p53iKO mice were notably smaller than in the control littermates (Fig. 3*G*), which was consistent with the reduced size of adipocytes in these adipose tissues. Moreover, the ratios between the weight of iWAT/eWAT depots and the total body weight were lower in aged Adipoq-p53iKO mice than in the control littermates (Fig. 3*H*), suggesting reduced adiposity after p53 ablation in aged mice. In adult humans, an increase of adiposity (particularly central/abdominal adiposity) and visceral adipose hypertrophy are closely associated with insulin resistance (40). In line with the reduced adiposity and size of white adipocytes, aged Adipoq-p53iKO mice had significantly faster glucose clearance in the IPGTT and IPITT (Fig. 3*I*, *J*). Thus, p53 ablation in aged adipose tissues benefited whole-body energy and glucose metabolism.

## Transient p53 inhibition by pifithrin-α mimicked the beneficial effects of inducible p53 ablation

Because genetic ablation of p53 was sufficient to reinstate WAT beiging and led to beneficial effects in aged mice, we further investigated the effect of transient p53 inhibition through a pharmacological approach. Pifithrin-α is a potent inhibitor of the transcriptional activation function of p53 (41). The choice of pifithrin-α was in line with the increase of p53 in the nucleus of aged adipocytes (Fig. 1*B*). To examine the effect of local administration, we administered pifithrin-α into subcutaneous iWAT of aged *C57BL/6* mice. Control aged *C57BL/6* mice were injected with the vehicle solution (1.6% DMSO). No sign of tumor formation was observed in either group of mice during or after pifithrin-α treatment.

To investigate the effect of pifithrin-α on cold-induced beige adipocyte formation, both pifithrin-α– and vehicle-injected young (8-wk-old) and aged (28-wk-old) mice were exposed to cold (4°C, 3 d). In cold-treated young mice, pifithrin-α administration did not increase the protein level of Ucp1 in iWAT compared to the DMSO control (**Fig. 4*A***). In cold-treated aged mice, however, pifithrin-α administration increased Ucp1 expression in iWAT compared to the DMSO control. In support of restored beiging capacity after pifithrin-α administration, real-time quantitative PCR revealed that the mRNA levels of the beige adipocyte markers *Ucp1*, *Pgc1α*, *Cidea*, *Cox8b*, and *Elovl3* in pifithrin-α–treated aged iWAT was 1.7–3.5-fold higher than in DMSO-treated aged iWAT (Fig. 4*B*). In addition, abundant multilocular $Ucp1^+$ beige adipocytes were observed in iWAT with pifithrin-α treatment but not in DMSO-injected iWAT (Fig. 4*C*). Similar to p53 genetic ablation, pifithrin-α–injected aged mice had increased total EE compared to control mice in both light and dark cycles (Fig. 4*D*). The RER of pifithrin-α–injected aged mice was also lower than in control mice in light cycles (Fig. 4*E*). When housed at 22°C, pifithrin-α–injected mice and control mice had comparable body weight within 28 d after treatment (Fig. 4*F*). The size of adipocytes in pifithrin-α–injected iWAT was overtly smaller than the control iWAT (Fig. 4*G*, *H*), mimicking the effect of p53 ablation (Fig. 2*G*). At room temperature (22°C), pifithrin-α–injected iWAT expressed 2–40-fold higher levels of the beige adipocyte markers *Ucp1*, *Pgc1α*, *Cidea*, *Cox8b*, and *Elovl3* than DMSO-injected control iWAT, suggestive of beige adipocyte formation, even with mild cold exposure (Fig. 4*I*). Similar to p53 ablation in aged mice, pifithrin-α administration in aged mice (at room temperature) also resulted in significantly faster glucose clearance in IPGTT and IPITT (Fig. 4*J*, *K*). Thus, transient pharmacological inhibition of p53 reinstated beige adipocyte formation in aged WAT and led to the same beneficial effects on energy and glucose metabolism as p53 genetic ablation.

## p53 ablation promoted mitochondria accumulation during beige adipocyte formation by attenuating mitophagy

Accumulating evidence indicates that autophagy impedes beige adipocyte recruitment (17–20). Consistent with this notion, the level of LC-3 lipidation (LC-3-II), an autophagy marker, decreased in beiging iWAT of young *C57BL/6* mice after cold exposure (4°C, 3 d; **Fig. 5*A***). Cold exposure in aged mice instead led to increased LC3-II (also LC3-I) expression, indicative of increased autophagy in beiging-defective iWAT with cold exposure. The decreased autophagy in beiging iWAT of young mice was accompanied with increased mitochondrial marker, *Pdh*, voltage-dependent anion channel 1 (*Vdac1*), heat shock protein (Hsp)60, and the electron transfer chain (ETC) protein, CoxIV (Fig. 5*B*). As expected, cold-induced beiging in young iWAT was also concomitant with an increase in Pgc1α expression, suggestive of a contribution of mitochondrial biogenesis to the accumulation of mitochondria during WAT beiging in young mice. Compared to control aged mice, aged Adipoq-p53iKO mice had increased expression levels of the mitochondrial markers Pdh, Vdac1, Hsp60, and CoxIV in iWAT after exposure to cold (4°C, 3 d), consistent with the restored beige adipocyte formation in this tissue. p53 ablation had only a minimal effect on Pgc1α expression, suggesting that dampened mitophagy contributes to the increase of mitochondria in aged Adipoq-p53iKO mice. Thus, we hypothesized that p53 impedes beige adipocyte formation by virtue of promoting mitophagy. To test this hypothesis, we compared the expression levels of the beige adipocyte marker Ucp1, the mitochondrial markers Vdac1, and CoxIV, the autophagy marker LC-3, and the mitophagy marker Parkin in aged Adipoq-p53iKO and control littermates after cold exposure (4°C, 3 d; Fig. 5*C*). p53 ablation decreased LC-3-II and Parkin levels but increased Ucp1, Vdac1, and CoxIV

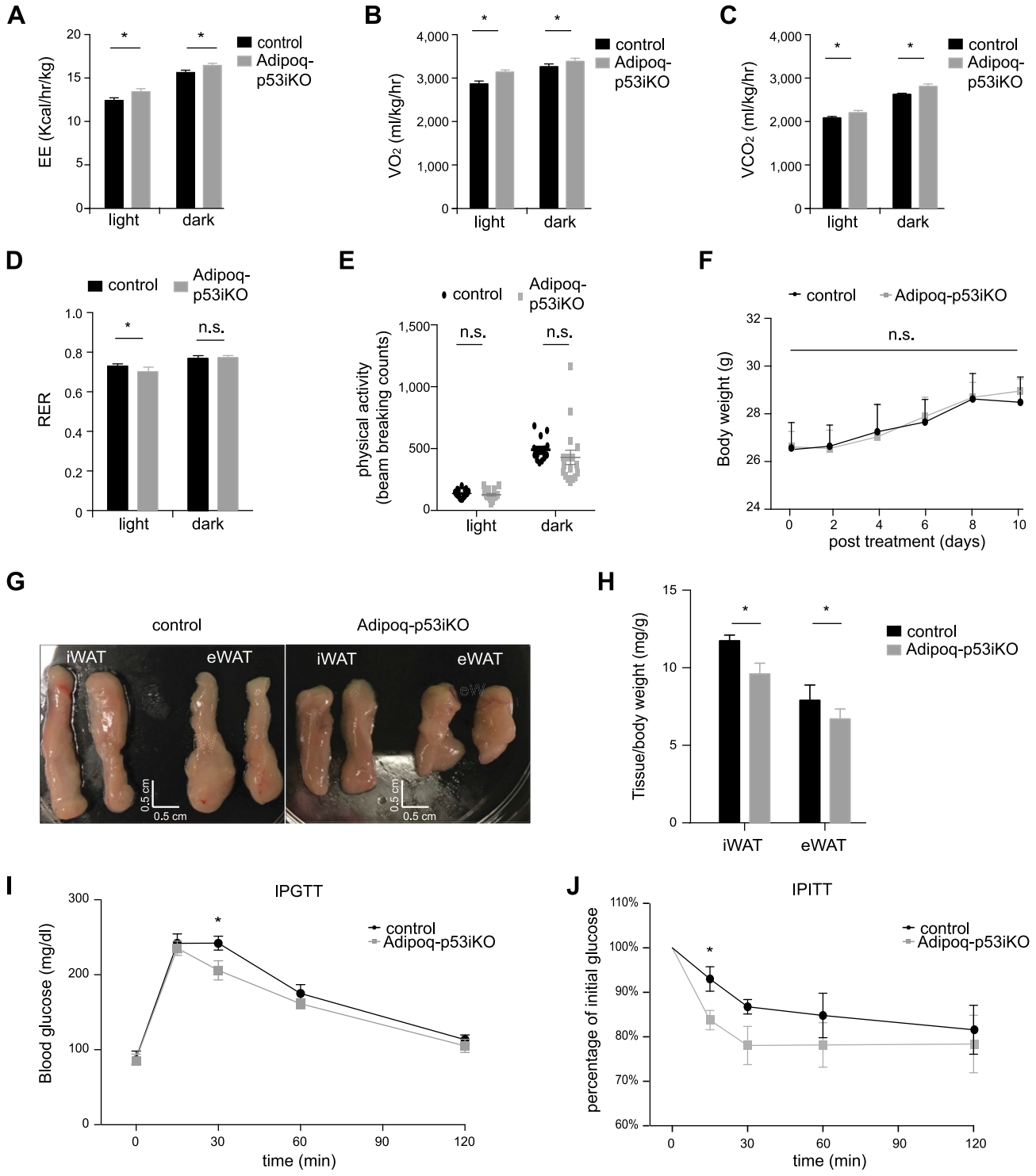


**Figure 3.** p53 ablation in aged adipose tissues augmented EE, reduced adiposity, and improved insulin sensitivity. *A–C*) EE (*A*), $Vo_2$ (*B*), and $Vco_2$ (*C*) of aged Adipoq-p53iKO mice and control littermates measured by indirect calorimetry (22°C; $n = 4$/group). *D*) RER of aged Adipoq-p53iKO mice and control littermates measured by indirect calorimetry (22°C; $n = 4$/group). *E*) Activities of aged Adipoq-p53iKO mice and control littermates during indirect calorimetry measurement (22°C; $n = 4$ per group). *F*) Body weight of aged Adipoq-p53iKO mice and control littermates after p53 ablation ($n = 6$/group). *G*) Representative images showing the sizes of iWAT and eWAT dissected from aged Adipoq-p53iKO mice and control littermates at 22°C. *H*) The ratios between the weight of iWAT and eWAT *vs.* body weight of aged Adipoq-p53iKO mice and control littermates ($n = 5$). *I, J*) IPGTTs (*I*) and IPITTs (*J*) of aged Adipoq-p53iKO mice and control littermates at 22°C ($n = 5$). Means ± SEM, by unpaired, 2-tailed Student's *t* test (*A, D, F, H, J*); n.s., not significant. $^*P < 0.05$, $^{**}P < 0.01$.

levels in iWAT of aged Adipoq-p53iKO mice, indicating that p53 ablation dampens mitophagy while inducing beiging in aged WAT. To confirm that dampened mitophagy is causative of restored beige adipocyte formation, we treated aged Adipoq-p53iKO mice with rapamycin, an inhibitor of mTORC1 and a potent inducer

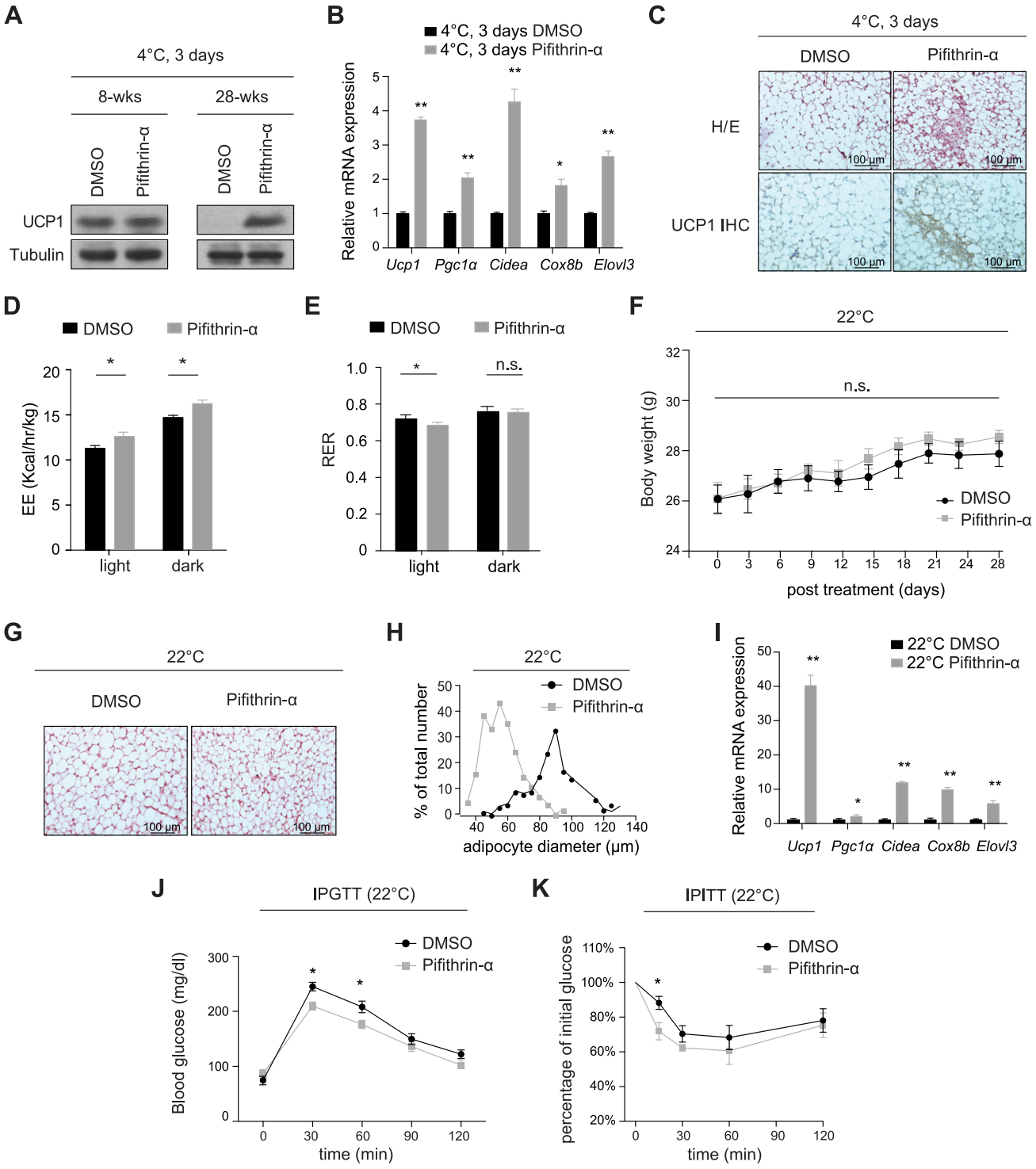


**Figure 4.** Transient p53 inhibition by pifithrin-α mimicked the beneficial effects of inducible p53 ablation. *A*) The expression levels of Ucp1 in iWAT of young (8-wk-old) and aged (28-wk-old) *C57BL/6J* mice after 4°C cold exposure (3 d) and pifithrin-α/DMSO injection. *B*) Relative mRNA levels of beige adipocyte markers *Ucp1*, *Pgc1α*, *Cidea*, *Cox8b*, and *Elovl3* in iWAT of aged Adipoq-p53iKO mice and control littermates after 4°C cold exposure (3 d). *C*) H&E staining and Ucp1 IHC of pifithrin-α/DMSO-injected iWAT from aged *C57BL/6J* mice after 4°C cold exposure (3 d). *D, E*) EE (*D*) and RER (*E*) of pifithrin-α/DMSO–treated aged *C57BL/6J* mice measured by indirect calorimetry ($n = 4$/group). *F*) Body weight of DMSO or pifithrin-α–injected, aged *C57BL/6J* mice during treatment ($n = 4$). *G*) H&E staining of aged iWAT injected with pifithrin-α or DMSO. *H*) Distributions of diameters of adipocytes in pifithrin-α/DMSO–injected aged iWAT. *I*) Relative mRNA levels of beige adipocyte markers *Ucp1*, *Pgc1α*, *Cidea*, *Cox8b*, and *Elovl3* in iWAT of pifithrin-α/DMSO–treated aged *C57BL/6J* mice. *J, K*) IPGTTs (*J*) and IPITTs (*K*) of pifithrin-α/DMSO–treated aged *C57BL/6J* mice ($n = 6$). Means ± SEM, by unpaired, 2-tailed Student's *t* test (*B, D, F, I–K*); n.s., not significant. $^*P < 0.05$, $^{**}P < 0.01$.

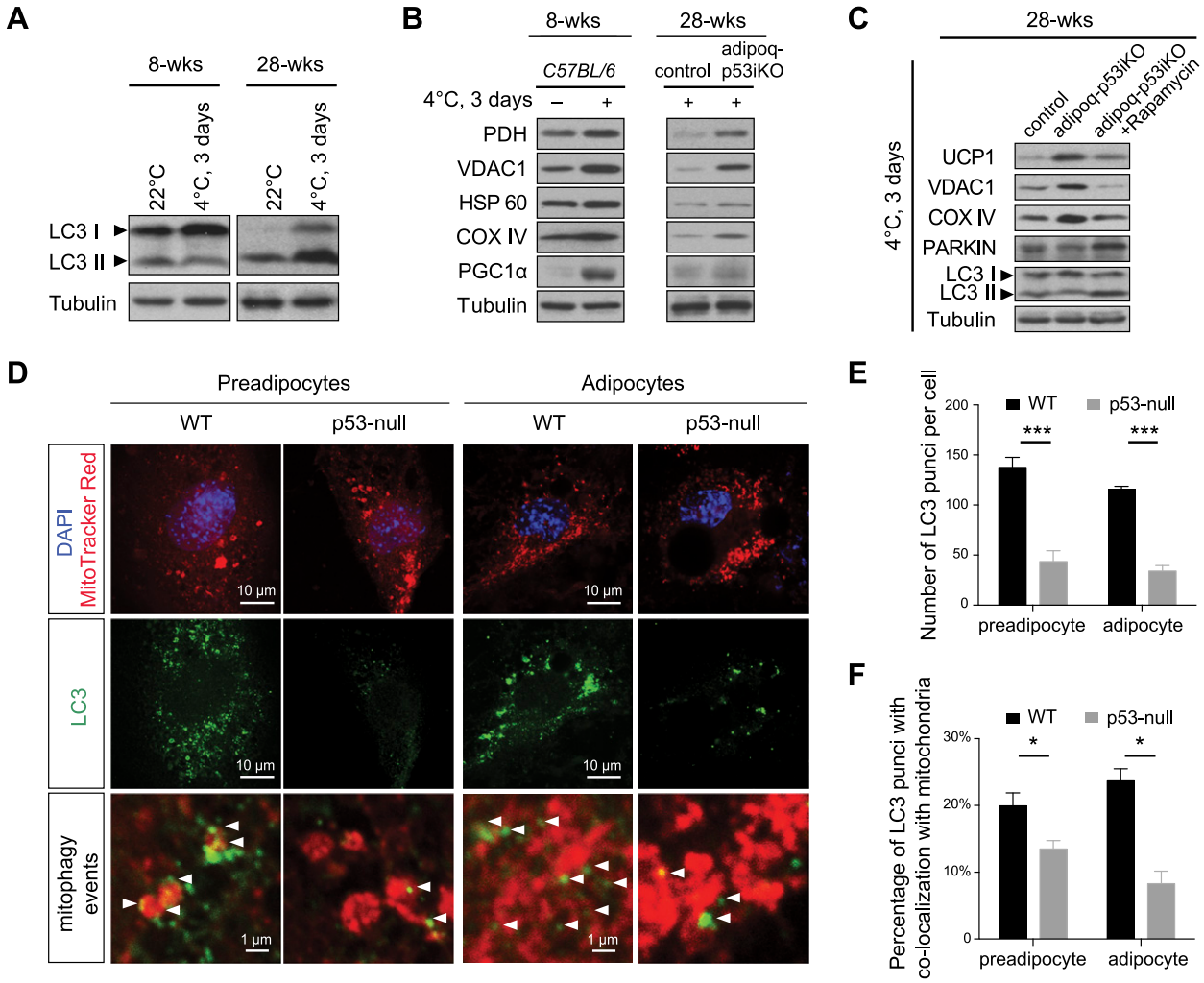


**Figure 5.** p53 ablation promoted mitochondria accumulation during beige adipocyte formation by attenuating mitophagy. *A*) Immunoblot analysis of LC3-I/II in iWAT of young (8-wk-old) and aged (28-wk-old) *C57BL/6J* mice at 22°C or after 4°C cold exposure (3 d). *B*) Left: immunoblot analysis of mitochondria makers Pdh, Vdac1, Hsp60, Cox-IV, and *Pgc1α* in iWAT of young *C57BL/6J* mice at 22°C or after 4°C cold exposure (3 d). Right: immunoblot analysis of same markers in iWAT of aged Adipoq-p53iKO mice and control littermates after 4°C cold exposure (3 d). *C*) Immunoblot analysis of Ucp1, Vdac1, CoxIV, LC3-I/II, and the mitophagy marker Parkin in iWAT of aged control mice, Adipoq-p53iKO mice, and Adipoq-p53iKO mice treated with rapamycin after 4°C cold exposure (3 d). *D*) Immunofluorescence staining of LC-3 (green), MitoTracker Red (red) and DAPI counterstaining (blue) in p53 WT and p53-null aged adipose progenitor cells and differentiated adipocytes. Arrowheads: mitophagy events in high-magnification fields. *E*) The number of total LC3 puncta of p53 WT and p53-null cells. *F*) The percentages of LC3 puncta colocalization with mitochondria staining *vs.* total LC3 puncta in p53 WT and p53-null cells. Means ± SEM (*E*, *F*); n.s., not significant by unpaired, 2-tailed Student's *t* test. $^*P < 0.05$; $^{**}P < 0.01$.

of autophagy and mitophagy (42). Rapamycin treatment augmented autophagy and mitophagy fluxes in iWAT of aged Adipoq-p53iKO mice, as evidenced by the increase in LC-3-II and Parkin levels. Importantly, Rapamycin-induced mitophagy also reduced Ucp1, Vdac1, and CoxIV levels, supporting the hypothesis that dampened mitophagy after p53 ablation promotes beige adipocyte formation.

To further validate that p53 induces mitophagy in aged adipocytes, we isolated p53 wild-type (WT) progenitor cells from aged iWAT and generated p53-null progenitor cells by CRISPR/Cas9-based mutagenesis. We compared mitophagic events in WT and p53-null progenitor cells and in differentiated adipocytes derived from these cells. Mitophagic events were identified as overlapped or juxtaposed localization of autophagosome (visualized as LC-3 puncta) with mitochondria (visualized by MitoTracker Red) after chloroquine treatment (43). We observed frequent mitophagic events in p53 WT progenitor cells and mature adipocytes (Fig. 5*D*). The number of LC-3 puncta in p53-null progenitor cells and mature adipocytes markedly decreased to ~30% of WT levels (Fig. 5*D*, *E*). In parallel with the reduction of LC-3 puncta, the percentage of LC-3 puncta that were overlapped or juxtaposed with mitochondria decreased in both p53-null progenitor cells (WT: 20% *vs.* p53-null: 13%) and p53-null mature adipocytes (WT: 25% *vs.* p53-null: 8%; Fig. 5*F*). These data support that p53 enhances mitophagy in aged adipocytes.

## DISCUSSION

This study revealed a previously unappreciated role of p53 in the impairment of beige adipocyte recruitment in aged

WAT. We provide evidence that the elevated p53 expression in aged adipocytes impeded the mitochondrial increase during white-to-beige adipocyte conversion. This negative impact was consistent with the function of p53 in promoting mitochondrial clearance by autophagy and mitophagy. Inducible ablation of p53 specifically in aged adipocytes reinstated the beiging capability in aged WATs, which led to increased EE as well as improved insulin sensitivity in aged mice.

It has been reported that p53 elevates in WATs after overfeeding of normal chow for 20 wk (in *Ay* mice) or after feeding of a high-fat high sucrose diet for 16 wk (25). The observation of increased p53 expression in WATs of 28-wk chow-fed mice in this study is consistent with these findings and suggests that WAT is particularly susceptible to aging. In aged WATs, the increase in p53 expression and its nuclear localization may be related to overnutrition-induced augmentation of mitochondrial bioenergetics, mTORC1 hyperactivity-induced mitochondrial biogenesis, and the consequent excessive ROS production (44, 45). Concordantly, many transcriptional targets of p53 are involved in the down-regulation of the mTORC1 pathway (*e.g.*, AMPK β-subunits, tuberculosis sclerosis complex (TSC)-2, phosphatase and tensin homolog) or the neutralization of ROS (*e.g.*, Sestrin1/2, and glutathione peroxidase 1) (31, 32, 46). Thus, the increase of p53 in aged WAT likely represents a compensatory mechanism to protect the genome from genotoxic ROS as a result of the aging-related deterioration of mitochondrial function. In line with this view, the repression of the mTORC1 pathway by p53 also facilitates the clearance of ROS-producing mitochondria *via* mitophagy, as previously demonstrated in mesenchymal stem cells (47). It is noteworthy, however, that p53-mediated restraint on mitochondrial bioenergetics is incompatible with the increase of energy metabolism during white-to-beige adipocyte conversion. Compared to white adipocytes with relatively inert metabolism, beige adipocytes develop high capacities in glucose, fatty acids, amino acids, and energy metabolism in support of NST, which is largely reliant on the extensive mitochondrial network (48). Indeed, this and previous studies demonstrated that the induction of mitophagy by rapamycin impairs beiging and thermogenesis in young and aged WAT (49). Thus, the observed repression of p53 in WATs after cold exposure in this study is in line with the needs to accumulate mitochondria and dampen mitophagy during the beiging process. The mitochondrial biogenesis master regulator *Pgc1α* consistently increased, whereas the autophagy marker LC3-II reduced during WAT beiging. Besides, autophagy and mitophagy decreased in p53-null adipose progenitor cells and adipocytes, as evidenced by the markedly reduced LC3 puncta and, particularly, the LC3 puncta surrounding the mitochondria. These findings are highly concordant with the reported function of p53 in transactivation of B-cell lymphoma (Bcl)-2 19-kDa interacting protein 3 (Bnip3) and uncoordinated-51–like autophagy activating kinase 1 (Ulk1), both of which are essential for the formation of autophagosome during autophagy and mitophagy (50, 51). Notably, the inhibition of the p53-downstream mTORC1 pathway impedes cold-induced WAT beiging and the increase in mitochondrial content (19, 20), further supporting that the repression of autophagy and mitophagy by either p53 inhibition or mTORC1 activation facilitates beige adipocyte recruitment. In addition to promoting autophagy and mitophagy, nuclear p53 has also been implicated in the transcriptional repressing of *Pgc1α* in brown adipocytes (37). p53 ablation in iWAT had a minimal effect on Pgc1α expression in aged mice in this study, suggesting the increase of mitochondrial content in this condition is principally attributable to dampened mitophagy.

Several studies have demonstrated that cold stress induces *de novo* beige adipogenic differentiation from perivascular progenitor cells that express *Myh11*, *Acta2*, Pdgfrα and -β, and SMA (52–55). In line with this finding, genetic ablation of p21 or Ink4a/Arf in $SMA^+$ adipose progenitor cells rescues cold-induced WAT beiging in 24-wk-old mice (11). As cell proliferation is concomitant with cold-induced beige differentiation of adipose progenitor cells in visceral fat depots (55), it is conceivable that a presumed increase of p53 in adipose progenitor cells and the consequent cellular senescence also impairs beige adipocyte formation in aged eWAT. In this study, the genetic depletion of p53 in 28-wk-old Adipoq-p53iKO mice also resulted in markedly increased WAT beiging after cold exposure. However, it is noteworthy that the p53 depletion in this study specifically affected Adiponectin-positive adipocytes, rather than adipose progenitor cells (38, 56). Thus, the restoration of beiging potential in this study essentially reflects intrinsic impairment of white-to-beige conversion in aged white adipocytes—a defect that has not been investigated before. Of note, a recent study revealed that beige adipocytes formed within inguinal WAT upon cold stress are exclusively derived from Adiponectin-positive uniocular adipocytes (57). Concordantly, the depletion of p53 in Adiponectin-positive adipocytes elicited a more pronounced effect within inguinal WAT than in epididymal WAT (Fig. 2*F*). Thus, p53-dependent cellular senescence in adipose progenitor cells and mature adipocytes may have variable contributions to the beiging defect in different fat depots but jointly entail WAT aging.

The data in this study indicate that inducible p53 depletion in aged adipocytes improved insulin sensitivity, which is highly consistent with observations from constitutive p53 ablation in the whole body or specifically in adipose tissues (25, 37). The reappearance of beige adipocytes in WATs conceivably contributed to the improved insulin sensitivity in aged Adipoq-p53iKO mice. However, it is also possible that p53 ablation ameliorates insulin resistance *via* pathways independent of beige adipocyte formation (58, 59). From the perspective of energy homeostasis, the restoration of WAT beiging represents an attractive strategy of clinical significance, in that the augmentation of EE and amelioration of white adipocyte hypertrophy, as observed in this study, may eliminate a rudimentary cause of WAT insulin resistance. Prolonged p53 inhibition/ablation conceivably leads to deleterious effects and raises risks of tumorigenesis. The transient inhibition of p53's transactivation activity in the nucleus by pifithrin-α conferred the same beneficial effects as p53

ablation in aged iWAT. The findings in this study warrant further investigation of molecular mechanisms underlying p53 and mitophagy in beige adipocyte recruitment and the defective signaling in aging, which may illuminate novel therapeutic strategies for metabolic syndrome. FJ

## ACKNOWLEDGMENTS

The authors thank Dr. Jarrod Call (The University of Georgia) for constructive discussion of the project. Research reported in this publication was supported by the U.S. National Institutes of Health, National Institute of Arthritis and Musculoskeletal and Skin Diseases Grant 1R01AR070178, and American Heart Association Grant-in-Aid 17GRNT33700260 (to H.Y.). The content is solely the responsibility of the authors and does not necessarily represent the official views of the NIH or American Heart Association. The authors declare no conflicts of interest.

## AUTHOR CONTRIBUTIONS

H. Yin designed the research; W. Fu analyzed the data; W. Fu, Y. Liu, and C. Sun performed the research; and W. Fu and H. Yin wrote the paper.

## REFERENCES

1. Harms, M., and Seale, P. (2013) Brown and beige fat: development, function and therapeutic potential. *Nat. Med.* **19**, 1252–1263
2. Cypess, A. M., Lehman, S., Williams, G., Tal, I., Rodman, D., Goldfine, A. B., Kuo, F. C., Palmer, E. L., Tseng, Y. H., Doria, A., Kolodny, G. M., and Kahn, C. R. (2009) Identification and importance of brown adipose tissue in adult humans. *N. Engl. J. Med.* **360**, 1509–1517
3. Wu, J., Boström, P., Sparks, L. M., Ye, L., Choi, J. H., Giang, A. H., Khandekar, M., Virtanen, K. A., Nuutila, P., Schaart, G., Huang, K., Tu, H., van Marken Lichtenbelt, W. D., Hoeks, J., Enerbäck, S., Schrauwen, P., and Spiegelman, B. M. (2012) Beige adipocytes are a distinct type of thermogenic fat cell in mouse and human. *Cell* **150**, 366–376
4. Sharp, L. Z., Shinoda, K., Ohno, H., Scheel, D. W., Tomoda, E., Ruiz, L., Hu, H., Wang, L., Pavlova, Z., Gilsanz, V., and Kajimura, S. (2012) Human BAT possesses molecular signatures that resemble beige/brite cells. *PLoS One* **7**, e49452
5. Saito, M., Okamatsu-Ogura, Y., Matsushita, M., Watanabe, K., Yoneshiro, T., Nio-Kobayashi, J., Iwanaga, T., Miyagawa, M., Kameya, T., Nakada, K., Kawai, Y., and Tsujisaki, M. (2009) High incidence of metabolically active brown adipose tissue in healthy adult humans: effects of cold exposure and adiposity. *Diabetes* **58**, 1526–1531
6. Van der Lans, A. A., Hoeks, J., Brans, B., Vijgen, G. H., Visser, M. G., Vosselman, M. J., Hansen, J., Jörgensen, J. A., Wu, J., Mottaghy, F. M., Schrauwen, P., and van Marken Lichtenbelt, W. D. (2013) Cold acclimation recruits human brown fat and increases nonshivering thermogenesis. *J. Clin. Invest.* **123**, 3395–3403
7. Lee, P., Smith, S., Linderman, J., Courville, A. B., Brychta, R. J., Dieckmann, W., Werner, C. D., Chen, K. Y., and Celi, F. S. (2014) Temperature-acclimated brown adipose tissue modulates insulin sensitivity in humans. *Diabetes* **63**, 3686–3698
8. Cypess, A. M., Weiner, L. S., Roberts-Toler, C., Franquet Elía, E., Kessler, S. H., Kahn, P. A., English, J., Chatman, K., Trauger, S. A., Doria, A., and Kolodny, G. M. (2015) Activation of human brown adipose tissue by a β3-adrenergic receptor agonist. *Cell Metab.* **21**, 33–38
9. Heaton, J. M. (1972) The distribution of brown adipose tissue in the human. *J. Anat.* **112**, 35–39
10. Rogers, N. H., Landa, A., Park, S., and Smith, R. G. (2012) Aging leads to a programmed loss of brown adipocytes in murine subcutaneous white adipose tissue. *Aging Cell* **11**, 1074–1083
11. Berry, D. C., Jiang, Y., Arpke, R. W., Close, E. L., Uchida, A., Reading, D., Berglund, E. D., Kyba, M., and Graff, J. M. (2017) Cellular aging contributes to failure of cold-induced beige adipocyte formation in old mice and humans [published correction in Cell Metab. (2017) 24, 481]. *Cell Metab.* **25**, 166–181
12. Cinti, S. (2002) Adipocyte differentiation and transdifferentiation: plasticity of the adipose organ. *J. Endocrinol. Invest.* **25**, 823–835
13. Mizushima, N., Levine, B., Cuervo, A. M., and Klionsky, D. J. (2008) Autophagy fights disease through cellular self-digestion. *Nature* **451**, 1069–1075
14. Lemasters, J. J. (2005) Selective mitochondrial autophagy, or mitophagy, as a targeted defense against oxidative stress, mitochondrial dysfunction, and aging. *Rejuvenation Res.* **8**, 3–5
15. Wilson-Fritch, L., Burkart, A., Bell, G., Mendelson, K., Leszyk, J., Nicoloro, S., Czech, M., and Corvera, S. (2003) Mitochondrial biogenesis and remodeling during adipogenesis and in response to the insulin sensitizer rosiglitazone. *Mol. Cell. Biol.* **23**, 1085–1094
16. Goldman, S. J., Zhang, Y., and Jin, S. (2011) Autophagic degradation of mitochondria in white adipose tissue differentiation. *Antioxid. Redox Signal.* **14**, 1971–1978
17. Martinez-Lopez, N., Athonvarangkul, D., Sahu, S., Coletto, L., Zong, H., Bastie, C. C., Pessin, J. E., Schwartz, G. J., and Singh, R. (2013) Autophagy in Myf5+ progenitors regulates energy and glucose homeostasis through control of brown fat and skeletal muscle development. *EMBO Rep.* **14**, 795–803
18. Zhang, Y., Goldman, S., Baerga, R., Zhao, Y., Komatsu, M., and Jin, S. (2009) Adipose-specific deletion of autophagy-related gene 7 (atg7) in mice reveals a role in adipogenesis. *Proc. Natl. Acad. Sci. USA* **106**, 19860–19865
19. Liu, D., Bordicchia, M., Zhang, C., Fang, H., Wei, W., Li, J. L., Guilherme, A., Guntur, K., Czech, M. P., and Collins, S. (2016) Activation of mTORC1 is essential for β-adrenergic stimulation of adipose browning. *J. Clin. Invest.* **126**, 1704–1716
20. Yang, S. B., Lee, H. Y., Young, D. M., Tien, A. C., Rowson-Baldwin, A., Shu, Y. Y., Jan, Y. N., and Jan, L. Y. (2012) Rapamycin induces glucose intolerance in mice by reducing islet mass, insulin content, and insulin sensitivity. *J. Mol. Med. (Berl.)* **90**, 575–585
21. Altshuler-Keylin, S., Shinoda, K., Hasegawa, Y., Ikeda, K., Hong, H., Kang, Q., Yang, Y., Perera, R. M., Debnath, J., and Kajimura, S. (2016) Beige adipocyte maintenance is regulated by autophagy-induced mitochondrial clearance. *Cell Metab.* **24**, 402–419
22. Lu, X., Altshuler-Keylin, S., Wang, Q., Chen, Y., Henrique Sponton, C., Ikeda, K., Maretich, P., Yoneshiro, T., and Kajimura, S. (2018) Mitophagy controls beige adipocyte maintenance through a parkin-dependent and UCP1-independent mechanism. *Sci. Signal.* **11**, eaap8526
23. Soro-Arnaiz, I., Li, Q. O. Y., Torres-Capelli, M., Meléndez-Rodríguez, F., Veiga, S., Veys, K., Sebastian, D., Elorza, A., Tello, D., Hernansanz-Agustín, P., Cogliati, S., Moreno-Navarrete, J. M., Balsa, E., Fuertes, E., Romanos, E., Martínez-Ruiz, A., Enriquez, J. A., Fernandez-Real, J. M., Zorzano, A., De Bock, K., and Aragonés, J. (2016) Role of mitochondrial complex IV in age-dependent obesity. *Cell Reports* **16**, 2991–3002
24. Rodier, F., Campisi, J., and Bhaumik, D. (2007) Two faces of p53: aging and tumor suppression. *Nucleic Acids Res.* **35**, 7475–7484
25. Minamino, T., Orimo, M., Shimizu, I., Kunieda, T., Yokoyama, M., Ito, T., Nojima, A., Nabetani, A., Oike, Y., Matsubara, H., Ishikawa, F., and Komuro, I. (2009) A crucial role for adipose tissue p53 in the regulation of insulin resistance. *Nat. Med.* **15**, 1082–1087
26. Chen, C. Y., Abell, A. M., Moon, Y. S., and Kim, K. H. (2012) An advanced glycation end product (AGE)-receptor for AGEs (RAGE) axis restores adipogenic potential of senescent preadipocytes through modulation of p53 protein function. *J. Biol. Chem.* **287**, 44498–44507
27. Narita, M., Young, A. R., and Narita, M. (2009) Autophagy facilitates oncogene-induced senescence. *Autophagy* **5**, 1046–1047
28. Young, A. R., Narita, M., Ferreira, M., Kirschner, K., Sadaie, M., Darot, J. F., Tavaré, S., Arakawa, S., Shimizu, S., Watt, F. M., and Narita, M. (2009) Autophagy mediates the mitotic senescence transition. *Genes Dev.* **23**, 798–803
29. Jung, C. H., Ro, S. H., Cao, J., Otto, N. M., and Kim, D. H. (2010) mTOR regulation of autophagy. *FEBS Lett.* **584**, 1287–1295
30. Feng, Z., Zhang, H., Levine, A. J., and Jin, S. (2005) The coordinate regulation of the p53 and mTOR pathways in cells. *Proc. Natl. Acad. Sci. USA* **102**, 8204–8209
31. Budanov, A. V., and Karin, M. (2008) p53 target genes sestrin1 and sestrin2 connect genotoxic stress and mTOR signaling. *Cell* **134**, 451–460
32. Feng, Z., Hu, W., de Stanchina, E., Teresky, A. K., Jin, S., Lowe, S., and Levine, A. J. (2007) The regulation of AMPK beta1, TSC2, and PTEN

expression by p53: stress, cell and tissue specificity, and the role of these gene products in modulating the IGF-1-AKT-mTOR pathways. *Cancer Res.* **67**, 3043–3053
33. Tasdemir, E., Maiuri, M. C., Galluzzi, L., Vitale, I., Djavaheri-Mergny, M., D'Amelio, M., Criollo, A., Morselli, E., Zhu, C., Harper, F., Nannmark, U., Samara, C., Pinton, P., Vicencio, J. M., Carnuccio, R., Moll, U. M., Madeo, F., Paterlini-Brechot, P., Rizzuto, R., Szabadkai, G., Pierron, G., Blomgren, K., Tavernarakis, N., Codogno, P., Cecconi, F., and Kroemer, G. (2008) Regulation of autophagy by cytoplasmic p53. *Nat. Cell Biol.* **10**, 676–687
34. Lusk, G. (1928). *The Elements of the Science of Nutrition*, 4th ed., W. B. Saunders, Philadelphia
35. Hall, B. M., Balan, V., Gleiberman, A. S., Strom, E., Krasnov, P., Virtuoso, L. P., Rydkina, E., Vujcic, S., Balan, K., Gitlin, I. I., Leonova, K. I., Consiglio, C. R., Gollnick, S. O., Chernova, O. B., and Gudkov, A. V. (2017) p16(Ink4a) and senescence-associated β-galactosidase can be induced in macrophages as part of a reversible response to physiological stimuli. *Aging (Albany N.Y.)* **9**, 1867–1884
36. Minamino, T., and Komuro, I. (2007) Vascular cell senescence: contribution to atherosclerosis. *Circ. Res.* **100**, 15–26
37. Hallenborg, P., Fjære, E., Liaset, B., Petersen, R. K., Murano, I., Sonne, S. B., Falkerslev, M., Winther, S., Jensen, B. A., Ma, T., Hansen, J. B., Cinti, S., Blagoev, B., Madsen, L., and Kristiansen, K. (2016) p53 regulates expression of uncoupling protein 1 through binding and repression of PPARγ coactivator-1α. *Am. J. Physiol. Endocrinol. Metab.* **310**, E116–E128
38. Lee, K. Y., Russell, S. J., Ussar, S., Boucher, J., Vernochet, C., Mori, M. A., Smyth, G., Rourk, M., Cederquist, C., Rosen, E. D., Kahn, B. B., and Kahn, C. R. (2013) Lessons on conditional gene targeting in mouse adipose tissue. *Diabetes* **62**, 864–874
39. Wu, J., Cohen, P., and Spiegelman, B. M. (2013) Adaptive thermogenesis in adipocytes: is beige the new brown? *Genes Dev.* **27**, 234–250
40. Patel, P., and Abate, N. (2013) Body fat distribution and insulin resistance. *Nutrients* **5**, 2019–2027
41. Komarov, P. G., Komarova, E. A., Kondratov, R. V., Christov-Tselkov, K., Coon, J. S., Chernov, M. V., and Gudkov, A. V. (1999) A chemical inhibitor of p53 that protects mice from the side effects of cancer therapy. *Science* **285**, 1733–1737
42. Raught, B., Gingras, A. C., and Sonenberg, N. (2001) The target of rapamycin (TOR) proteins. *Proc. Natl. Acad. Sci. USA* **98**, 7037–7044
43. Kliosnky, D., Abdelmohsen, K., Abe, A., Abedin, M. J., Abeliovich, H., …and Zughaier, S. M. (2016) Guidelines for the use and interpretation of assays for monitoring autophagy (3rd edition). *Autophagy* **12**, 1–222
44. Morita, M., Gravel, S. P., Chénard, V., Sikström, K., Zheng, L., Alain, T., Gandin, V., Avizonis, D., Arguello, M., Zakaria, C., McLaughlan, S., Nouet, Y., Pause, A., Pollak, M., Gottlieb, E., Larsson, O., St-Pierre, J., Topisirovic, I., and Sonenberg, N. (2013) mTORC1 controls mitochondrial activity and biogenesis through 4E-BP-dependent translational regulation. *Cell Metab.* **18**, 698–711
45. Ahima, R. S. (2009) Connecting obesity, aging and diabetes. *Nat. Med.* **15**, 996–997
46. Sablina, A. A., Budanov, A. V., Ilyinskaya, G. V., Agapova, L. S., Kravchenko, J. E., and Chumakov, P. M. (2005) The antioxidant function of the p53 tumor suppressor. *Nat. Med.* **11**, 1306–1313
47. Ma, Y., Qi, M., An, Y., Zhang, L., Yang, R., Doro, D. H., Liu, W., and Jin, Y. (2018) Autophagy controls mesenchymal stem cell properties and senescence during bone aging. *Aging Cell* **17**, e12709
48. Ikeda, K., Maretich, P., and Kajimura, S. (2018) The common and distinct features of brown and beige adipocytes. *Trends Endocrinol. Metab.* **29**, 191–200
49. Tran, C. M., Mukherjee, S., Ye, L., Frederick, D. W., Kissig, M., Davis, J. G., Lamming, D. W., Seale, P., and Baur, J. A. (2016) Rapamycin blocks induction of the thermogenic program in white adipose tissue. *Diabetes* **65**, 927–941
50. Wang, E. Y., Gang, H., Aviv, Y., Dhingra, R., Margulets, V., and Kirshenbaum, L. A. (2013) p53 mediates autophagy and cell death by a mechanism contingent on Bnip3. *Hypertension* **62**, 70–77
51. Gao, W., Shen, Z., Shang, L., and Wang, X. (2011) Upregulation of human autophagy-initiation kinase ULK1 by tumor suppressor p53 contributes to DNA-damage-induced cell death. *Cell Death Differ.* **18**, 1598–1607
52. Berry, D. C., Jiang, Y., and Graff, J. M. (2016) Mouse strains to study cold-inducible beige progenitors and beige adipocyte formation and function. *Nat. Commun.* **7**, 10184
53. Long, J. Z., Svensson, K. J., Tsai, L., Zeng, X., Roh, H. C., Kong, X., Rao, R. R., Lou, J., Lokurkar, I., Baur, W., Castellot, J. J., Jr., Rosen, E. D., and Spiegelman, B. M. (2014) A smooth muscle-like origin for beige adipocytes. *Cell Metab.* **19**, 810–820
54. Vishvanath, L., MacPherson, K. A., Hepler, C., Wang, Q. A., Shao, M., Spurgin, S. B., Wang, M. Y., Kusminski, C. M., Morley, T. S., and Gupta, R. K. (2016) Pdgfrβ+ mural preadipocytes contribute to adipocyte hyperplasia induced by high-fat-diet feeding and prolonged cold exposure in adult mice. *Cell Metab.* **23**, 350–359
55. Lee, Y. H., Petkova, A. P., Mottillo, E. P., and Granneman, J. G. (2012) In vivo identification of bipotential adipocyte progenitors recruited by β3-adrenoceptor activation and high-fat feeding. *Cell Metab.* **15**, 480–491
56. Jeffery, E., Berry, R., Church, C. D., Yu, S., Shook, B. A., Horsley, V., Rosen, E. D., and Rodeheffer, M. S. (2014) Characterization of Cre recombinase models for the study of adipose tissue. *Adipocyte* **3**, 206–211
57. Lee, Y. H., Petkova, A. P., Konkar, A. A., and Granneman, J. G. (2015) Cellular origins of cold-induced brown adipocytes in adult mice. *FASEB J.* **29**, 286–299
58. Itahana, Y., and Itahana, K. (2018) Emerging roles of p53 family members in glucose metabolism. *Int. J. Mol. Sci.* **19**, E776
59. Kung, C. P., and Murphy, M. E. (2016) The role of the p53 tumor suppressor in metabolism and diabetes. *J. Endocrinol.* **231**, R61–R75

*Received for publication March 25, 2018.*
*Accepted for publication July 9, 2018.*